Theory of Secondary Domain Structures in Disordered Multiblock Copolymers

Alexander N. Semenov*

Department of Applied Mathematics, University of Leeds, Leeds LS2 9JT, U.K.

Alexei E. Likhtman†

Physics Department, Moscow State University, Moscow 117234, Russia

Received July 2, 1998; Revised Manuscript Received September 28, 1998

ABSTRACT: Microdomain structures in multicblock copolymers are studied theoretically with the focus on the effect of block polydispersity. It is shown that even weak polydispersity results in formation of secondary domains characterized by an internal primary microstructure. These secondary structures are predicted near the transition lines between different primary morphologies. The secondary domain size is very sensitive to temperature, polydispersity degree, etc. The secondary morphologies resulting from competition between disordered and spherical (cylindrical and lamellar) primary structures are studied in detail.

1. Introduction

One of the most attractive features of block copolymers (i.e., polymers formed by two kinds of monomers, say A and B) is their ability to form periodic domain structures.[1,2] The simplest system that received most of the theoretical attention[3−11] is a diblock-copolymer melt. Other polymer chain structures such as multiblock copolymers have been studied more recently.[12−16] In practice, blocks are always characterized by some molecular weight distribution, i.e., polydispersity. In the case of diblock copolymers the effect of polydispersity results in macroscopic phase separation between microdomain structures with different morphologies (i.e., different domain shape/symmetry).[6−11] Theory of microdomain structures in random copolymers and in highly polydisperse multiblock copolymers has been developed in refs.[17−33]

Recently it was shown that the effect of polydispersity in multiblock copolymers is more delicate giving rise to formation of secondary periodic structures.[27] These structures are stable in the regions where different primary microdomain morphologies tend to coexist; in a way they replace two-phase (macroseparated) states of polydisperse diblock-copolymer systems. To illustrate the main idea, let us consider the microphase separation (disorder to order transition) in slightly polydisperse ABAB... multiblock copolymers assuming that the number of blocks per chain is very large. Longer A and B blocks exhibit stronger tendency for segregation (akin to homopolymer blends which become more incompatible as the molecular weight increases), so they form a (primary) microphase-separated structure more readily than shorter blocks. Therefore in the regime where the two structures, homogeneous (disordered) and microdomain (ordered), are competitive (i.e., are characterized by nearly equal free energies), the system will tend to form two phases: ordered, which is rich in longer blocks, and disordered, which is rich in shorter blocks. Hence biphasic windows are predicted for bidisperse (polydisperse) *di*block copolymers.[9,11] In the case of long *multi*block copolymers, the longer and shorter blocks are typically connected within the same polymer chain, so they cannot separate macroscopically. Hence there is a possibility of *secondary* domain structures like, say, alternating disordered and ordered layers (Figure 1). The period of the secondary structure, Λ, is expected to be much larger than the primary period, L; in general the two structures are also incommensurable (different secondary morphologies are possible, see below Figures 4 and 7). The aim of the present paper is to study the secondary morphologies in some detail focusing on the weak segregation limit[3] where a quantitative analytical consideration is possible. The free energy is analyzed in the next two sections. The secondary structures related to transitions from disorder to spherical and from cylindrical to lamellar primary morphologies are described in sections 4 and 5; the results are discussed in section 6.

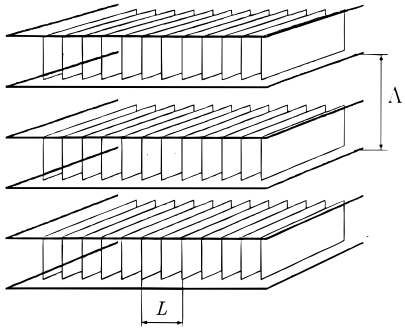

Figure 1. Lamellar secondary structure: alternating ordered and disordered lamellar sheets. The period of the secondary structure, Λ, is expected to be much larger than the primary period, L.

2. The Free Energy

2.1. The Model. We consider a melt of ABAB... multiblock copolymers, the number of blocks per chain, $n \to \infty$. The average number of monomers per block is $\langle n_A \rangle = n(1 + 2\epsilon)$, $\langle n_B \rangle = n(1 - 2\epsilon)$. We assume that $n \gg 1$ (this assumption ensures that fluctuation effects are

* To whom correspondence should be addressed.
† Present address: University of Leeds.

10.1021/ma981044j CCC: $15.00
Published on Web 11/26/1998

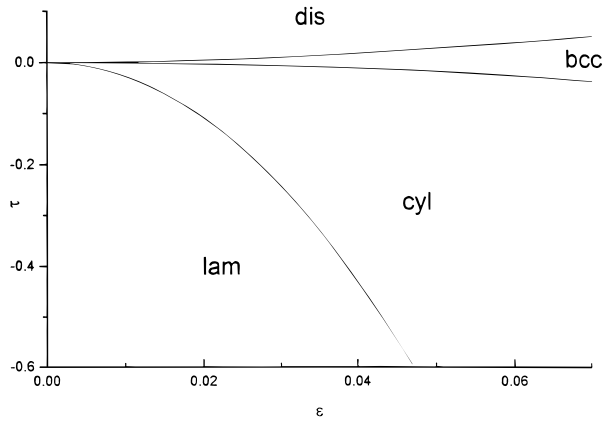

Figure 2. Phase diagram of a multicblock copolymer melt near the critical point[13] in variables ϵ (composition asymmetry) and τ (reduced temperature). Note disordered (dis), 3d periodic body centered cubic (bcc), 2d hexagonal "cylindrical" (cyl), and 1d lamellar (lam) morphologies.

weak,[4] and so they are neglected here: a mean field theory is presented below; the fluctuation effects are briefly discussed in section 6) and that $\epsilon \ll 1$; i.e., the compositional asymmetry is small. We also assume an effective repulsion between A and B monomers which is accounted for by the standard Flory excess free energy (per unit volume), $f_{int} = k_B T\chi\phi_A\phi_B/v$, where $\phi_{A,B}$ are the local volume concentrations of A and B monomers, v is the monomer volume, and χ is the Flory interaction parameter (the reference state is that of complete separation of A and B monomers, i.e., two phases: pure A and pure B). The melt is assumed to be incompressible: $\phi_A + \phi_B = 1$. Hence f_{int} can be represented as $f_{int} = (k_B T/nv)(\chi n)\phi_A(1 - \phi_A) = c_0 + c_1\phi_A - (\chi n)(\phi_A - (1 + 2\epsilon)/2)^2$. Here c_0 and c_1 are constants, and $(1 + 2\epsilon)/2$ is the average fraction of A monomers in the system. The prefactor $k_B T/nv$ is considered as the energy density unit and is omitted here and below. The first two terms in the right-hand side of the last equation ($c_0 + c_1\phi_A$) are irrelevant, as after integration over the whole volume they produce a constant which does not depend on the spatial structure of the system. Thus, omitting these terms we get

$$f_{int}(\phi_A) = -(\chi n)\left(\phi_A - \frac{1 + 2\epsilon}{2}\right)^2 \qquad (1)$$

The polydispersity degree of the blocks can be characterized by the parameters $\delta_A = \langle \delta n_A^2\rangle/\langle n_A\rangle^2$, $\delta_B = \langle \delta n_B^2\rangle/\langle n_B\rangle$, where $\delta n_A \equiv n_A - \langle n_A\rangle$; note that the standard ratio of the weight-average to number-average block A molecular weights is equal to $1 + \delta_A$ ($1 + \delta_B$ in the case of B blocks). We assume weak polydispersity: $\delta_{A,B} \ll 1$.

2.2 The Monodisperse Case. The monodisperse case ($\delta_A = \delta_B = 0$) corresponds to the regular multiblock copolymer system which undergoes a microphase separation transition if χn exceeds some critical (spinodal) value $X^*(\epsilon)$; the critical point corresponds to $\epsilon = 0$ and $\chi n = X^*(0) \simeq 7.55$ (see ref 12; here we assume equal statistical segments of A and B blocks: $a_A = a_B = a$). The phase behavior of the system near the critical point (i.e., in the weak segregation regime) is similar[13] to that for diblock copolymer melt as predicted by Leibler;[3] the schematic phase diagram is shown in Figure 2. The phase behavior is independent of the sign of the asymmetry parameter ϵ, so here and below we assume that $\epsilon > 0$. Note disordered (dis), 3d periodic body centered cubic (bcc), 2d hexagonal "cylindrical" (cyl), and 1d lamellar (lam) morphologies. Other structures such as gyroid bicontinuous morphology are not stable close enough to the critical point.[2]

The free energy of the disordered (homogeneous) system is a sum of the ideal-gas term and the free energy of monomer interactions f_{int}. The entropic ideal-gas free energy is negligible since copolymer chains are very long. On the other hand f_{int}, eq 1, also vanishes since $\phi_A \equiv (1 + 2\epsilon)/2$ in the disordered state, i.e.,

$$f_{dis} = 0 \qquad (2)$$

The free energy of a generic ordered phase is $f_{ord} = f_{dis} + f_1$, where f_1 depends on the monomer distributions, i.e., on the order parameter field $\psi(r) = \phi_A(r) - (1 + 2\epsilon)/2$.

$$f_1 = \frac{1}{2}\hat{\gamma}_2\psi^2 + \frac{1}{3!}\hat{\gamma}_3\psi^3 + \frac{1}{4!}\hat{\gamma}_4\psi^4 + \ldots \qquad (3)$$

where $\hat{\gamma}_2\psi^2$ is a shortcut for $\int\gamma_2(r')\psi(r)\psi(r + r')\,dr'$, etc. In the disordered phase $\psi(r) \equiv 0$, and so $f_1 = 0$. The expansion, eq 3, is useful in the weak segregation limit (WSL) when ψ^2 is small; in this regime the Fourier image of the vertex function γ_2 can be approximated as (note that the prefactor $k_B T/nv$ is omitted) $\gamma_2(q) = \tau + C(q - q^*)^2$, where $C \sim R_n^2 = na^2$, $\tau = 2[X^*(\epsilon) - \chi n]$ is the relative distance to the spinodal, $|\tau| \ll 1$, and q^* is the critical wave vector related to the period of the microdomain structure $L = 2\pi/q^*$. In the WSL, the structural period is of the order of the Gaussian block size R_n: $L \sim R_n = n^{1/2}a$. Minimizing f_1 with respect to $\psi(r)$ we get the equilibrium free energy $f_1 = f_1(\tau)$. Transitions between disordered and ordered primary superstructures all occur at $|\tau| \sim \epsilon^2 \ll 1$.

2.3. The Local Effect of Polydispersity. For regular block copolymers the vertex functions γ_2, γ_3, ... depend on the block lengths, n_{A0} and n_{B0}. With polydispersity the situation is more complicated: these functions depend on the whole sequence of block lengths $\{n_{A1}, n_{B1}, n_{A2}, n_{B2}, \ldots\}$ along the chain (in the limit $n \to \infty$ we can think of just one extremely long block-copolymer chain filling the whole space). In the case of weak polydispersity the vertex functions can be expanded in a series of $\delta n_{ji} = n_{ji} - n_{j0}$, e.g.

$$\gamma_2 = \gamma_2^{(0)} + \sum C_{ji}\delta n_{ji} + \ldots$$
$$j = \text{A, B};\ i = 1, 2, \ldots \qquad (4)$$

where $\gamma_2^{(0)}$ corresponds to the monodisperse system ($\delta = 0$), i.e., regular block copolymer. Obviously C_{ji} does not depend on i in the case of long chains (i.e., negligible end effects), so that eq 4 becomes (we omit quadratic and higher-order terms):

$$\gamma_2 = \gamma_2^{(0)} + \Delta\gamma_2; \quad \Delta\gamma_2 \simeq C_A\sum\delta n_{Ai} + C_B\sum\delta n_{Bi}$$

i.e., the vertex functions depend on the deviation of the *average* block length from the reference values: $\langle\delta n_A\rangle = \langle n_A\rangle - n_{A0}$ and $\langle\delta n_B\rangle$. The value $\langle\delta n_A\rangle$ is identically zero when averaged over the whole system. However in general we should consider a structurally heterogeneous system when, e.g., longer blocks are selectively accumulated in some parts of the volume (reflecting coexistence of different primary morphologies, i.e., the

secondary superstructure). Then the free energy density is determined by the *local* values of the vertex functions (γ_2, ...) which in turn are determined by the *locally* averaged block lengths $\langle n_A\rangle_{local}$, i.e., $f_1 = f_1(\tau,\varphi_A,\varphi_B)$, where we introduce two new order parameter fields, φ_A and φ_B:

$$\langle n_A\rangle_{local} = n(1 + 2\epsilon + \varphi_A); \qquad \langle n_B\rangle_{local} = n(1 - 2\epsilon + \varphi_B) \quad (5)$$

Here $\langle\rangle_{local}$ means averaging over a scale larger than the size $L = 2\pi/q^*$ of the primary microdomain structure (note that L is also the scale of nonlocality of the vertex functions) but smaller than the size of secondary domains Λ (below we show that Λ is always much larger than L, so this averaging procedure makes sense).

The function $f_1(\tau,\varphi_A,\varphi_B)$ can be easily found using eq 4 and similar equations for γ_3 and γ_4 (note that in general case the first-order parameter is defined as $\psi(r) = \phi_A(r) - \langle\phi_A\rangle_{local}$, i.e., $\langle\psi\rangle_{local} \equiv 0$). The corrections to all vertex functions, $\Delta\gamma_{2,3,4}$ are of order $\varphi_A + \varphi_B$; on the other hand the reference values (for $\varphi_A = \varphi_B = 0$) are very different, $\gamma_2 \sim \epsilon^2$, $\gamma_3 \sim \epsilon$, $\gamma_4 \sim 1$ (these estimates can be easily deduced using Leibler's approach;[3] remember that prefactor k_BT/nv is set to be unity), i.e., $\gamma_2 \ll \gamma_3 \ll \gamma_4$. Therefore the relative correction $\Delta\gamma_2/\gamma_2$ is much larger than relative corrections to other vertex functions, which thus can be neglected. Furthermore, the correction to γ_2 can be accounted for by replacing τ with its effective local value $\tau_{eff} = 2[X^*(\epsilon) - \chi\langle n\rangle_{local}]$, where $\langle n\rangle_{local} = (1/2)(\langle n_A\rangle_{local} + \langle n_B\rangle_{local}) = n(1 + \varphi)$

$$\varphi = \frac{\varphi_A + \varphi_B}{2} = \frac{\langle n\rangle_{local} - n}{n} \quad (6)$$

Note that

$$\int \varphi(r)\, d^3r = 0 \quad (7)$$

since the mean block length averaged over the whole system is equal to n. Note also that "fluctuations" of block lengths also generate a correction to the compositional parameter ϵ, $\Delta\epsilon = (\varphi_A - \varphi_B)/4$. However this correction is negligible since $X^*(\epsilon) = X^*(0) + \text{const}\ \epsilon^2$, i.e., no linear term in this ϵ-expansion. Thus in the first approximation (i.e. neglecting quadratic and higher-order terms) $\tau_{eff} \simeq \tau - 2X^*\varphi$, so that $f_1 \equiv f_1(\tau,\varphi_A,\varphi_B) \simeq f_1^{(0)}(\tau_{eff})$, where $f_1^{(0)}(\tau)$ is the free energy of the corresponding regular block-copolymer system. Using eq 3 and the theorem on small increments[34] we get

$$f_1 \simeq f_1^{(0)}(\tau) - h\varphi \quad (8)$$

where

$$h \equiv X^*\langle\psi^2\rangle_{local} \quad (9)$$

$h = 0$ for the disordered (homogeneous) state, $h \sim \epsilon^2$ for microphase separated morphologies (h is increasing along the sequence dis → bcc → cyl → lam).

The free energy f_{dis} of the background (disordered) state is determined by the local composition: $f_{dis} = f_{int}(\langle\phi_A\rangle_{local})$, and so f_{dis} depends on the order parameter fields:

$$f_{dis} = -(\chi n)\left(\frac{\varphi_A - \varphi_B}{4}\right)^2 \quad (10)$$

The total free energy per unit volume is (the meaning of the subscript "local" is clarified below)

$$f_{local} = f_{dis} + f_1 + f_\varphi \quad (11)$$

where f_1 is defined in eq 8 and f_φ is the entropic penalty related to a given "fluctuation" of the block lengths: $f_\varphi = -(k_BT/V_1)\ln P(\varphi_A, \varphi_B, V_1)$. Here $P(\varphi_A,\varphi_B,V_1)$ is the a priori probability that the average block lengths inside the subvolume V_1 are equal to those defined in eqs 5 (V_1 is much smaller than the total volume of the whole system; in fact V_1 can be defined as the volume related to local averaging). The probability distribution P must be nearly Gaussian since V_1 contains many blocks, i.e., f_φ must be a quadratic function of φ_A and φ_B: $f_\varphi = (1/2)(\kappa_{AA}\varphi_A^2 + 2\kappa_{AB}\varphi_A\varphi_B + \kappa_{BB}\varphi_B^2)$. The coefficients κ_{AA}, ... are related to the correlators $\langle\varphi_A^2\rangle$, ..., which in turn are determined by the polydispersity degrees, $\delta_{A,B}$. Assuming no correlations between the block lengths along the chain we get

$$f_\varphi = \frac{1}{4}\frac{1}{\delta_A}\varphi_A^2 + \frac{1}{4}\frac{1}{\delta_B}\varphi_B^2 \quad (12)$$

Obviously f_φ dominates over f_{dis} (see eq 10 since $\delta_{A,B} \ll 1$, i.e., the term f_{dis} can be neglected. Note that the entropic free energy f_φ ensures that the block length fluctuations are totally suppressed in the limit $\delta_{A,B} \to 0$ as it should be.

Note that the structural free energy f_1 depends essentially on a single combination φ, eq 6, of the order parameters φ_A and φ_B. As we are looking for the equilibrium free energy, we can exclude one of the order parameters by minimizing f_φ over φ_A, φ_B for a fixed φ. Thus we get

$$f_\varphi = \frac{1}{2}\kappa\varphi^2, \qquad \kappa = \frac{1}{\delta}, \qquad \delta = \frac{\delta_A + \delta_B}{2} \quad (13)$$

i.e., δ is the average block polydispersity degree. Using eqs 8, 10, and 11, we get

$$f_{local} \simeq \frac{1}{2}\kappa\varphi^2 - h\varphi + f_1^{(0)}(\tau) \quad (14)$$

2.4. Nonlocal Free Energy. The argument used above to derive the entropic free energy, f_φ, is strictly valid for block copolymers with molten disorder, i.e., when each block can change its molecular weight from time to time so as to generate the prescribed molecular weight distribution. In the case of fixed chemical structure of copolymer chains, i.e., quenched disorder (it is this case we are interested in), the situation is more complicated because of a possible coupling between the chain sequence and its spatial trajectory. Yet it can be shown that eq 13 is still valid with quenched disorder provided that the system being finite can exchange molecules with an infinite supply of polydisperse block copolymers.

However an important correction to eq 13 is expected if the order parameter φ is nonzero in a considerable fraction of a finite system. This correction will be referred to as nonlocal free energy since it depends not only on the order parameter field $\varphi(r)$ but also on the total volume of the system V. To illustrate the nature of the nonlocal free energy, let us consider the following simple example: $\varphi(r) = \varphi_0$ in half of a large but finite system $V = D^3$, and $\varphi(r) = -\varphi_0$ in the other half.

Obviously both halves must be filled by chain fragments of size $\sim D$, the number of blocks per fragment is $m \sim D^2/na^2$ if we assume unperturbed Gaussian statistics of the fragments. The average block length for the fragments in the first half is $n(1 + \varphi_0)$ and in the second half is $n(1 - \varphi_0)$. The probability to find an m-fragment with $\langle n \rangle = n(1 + \varphi_0)$ is proportional to $\exp(-m\varphi_0^2/2\delta)$, i.e., it is exponentially small if m is large enough. That is the fraction of m-fragments suitable for the first half might be exponentially small, i.e., these fragments cannot possibly fill half of the whole volume. The only way out of this contradiction is to assume that chain conformational statistics is perturbed (chain fragments are stretched), hence nonlocal free energy related to elasticity of chain fragments.

The nonlocal free energy can be calculated using the perturbation approach (i.e., expansion in series of the order parameter φ) similar to that suggested for random copolymers[17] (different modifications of this approach both involving replica trick and replica-free have been suggested more recently[18−21]). We omit the derivation here as it is identical to that presented originally[17] provided the standard order parameter ψ is replaced by φ. The result is

$$F_{\text{nloc}} = \frac{\kappa^2}{4V^3}\frac{2}{na^2}\sum_{q,q'}\frac{|\varphi_q|^2\,|\varphi_{q'}|^2}{q^2 + q'^2} \tag{15}$$

where $\varphi_q = \int \varphi(r) e^{-iqr}\, d^3r$, and the wave-vectors q, q' take all appropriate values defined by the volume V.

Equation 15 is valid if $\varphi_q \simeq 0$ for $qR_n \gtrsim 1$, which is true since the order parameter field by definition is smoothed over a scale larger than $R_n = n^{1/2}a$. Another condition is that φ must be small enough so that

$$\kappa\varphi^2\Lambda^2/(na^2) \ll 1 \tag{16}$$

otherwise higher-order terms might become important (here φ and Λ are the typical value and the typical scale associated with the field $\varphi(r)$).

We are now in a position to define the total free energy of a generic structure involving different morphologies in different parts of the system, i.e., secondary domain structure

$$F = F_{\text{local}} + F_{\text{nloc}} + F_{\text{intf}} \tag{17}$$

where $F_{\text{local}} = \int f_{\text{local}}\, d^3r$, f_{local} is defined in eq 14, and F_{intf} is the free energy of interfaces between secondary domains:

$$F_{\text{intf}} = \int \sigma(r)\, dA$$

Here $\sigma(r)$ is the interfacial tension which might depend on the local orientation of the interfacial area element dA and which is considered below.

3. Interfacial Tension

Weak polydispersity nearly does not affect the interfacial tension (note that σ corresponds to interfaces between the regions with different primary morphologies, i.e., σ is *not* the energy of primary interfaces between ordinary microdomains). Hence we calculate σ for $\delta = 0$, i.e., assuming a monodisperse system.

Let us consider first the dis/bcc interface (note that dis/lam interfaces has been studied analytically in refs 35 and 36). For bulk disordered phase $\psi \equiv 0$; bulk bcc phase is characterized by a set of six wave vectors that form a perfect tetrahedron plus six antiparallel vectors: $\{\mathbf{Q}_i,\ i = 1 \ldots 12\}$, $|\mathbf{Q}_i| = q^*$,

$$\psi(\mathbf{r}) = \sum_{i=1}^{12} A_i e^{i\mathbf{Q}_i\mathbf{r}} \tag{18}$$

where all the amplitudes are equal $A_i = A_0$ (see ref 3). The interfacial structure can be described by the functions $A_i(z)$, $A_i(z) \to 0$ for $z \to -\infty$, $A_i(z) \to A_0$ for $z \to \infty$; here we assume that interface is parallel to the xy plane, i.e., $z = 0$. The total free energy of (monodisperse) system is $F = \int f_1\, d^3r$; using eq 3 we get

$$F = \frac{1}{2}\sum_i \int_q \gamma_2(\mathbf{Q}_i + \mathbf{q})|A_i(\mathbf{q})|^2 + \frac{1}{3!}\sum_{\mathbf{Q}_i+\mathbf{Q}_j+\mathbf{Q}_l=0} \int_{\mathbf{q}_1+\mathbf{q}_2+\mathbf{q}_3=0} \gamma_3 A_i(\mathbf{q}_1)A_j(\mathbf{q}_2)A_l(\mathbf{q}_3) + \frac{1}{4!}\sum_{\mathbf{Q}_i+\mathbf{Q}_j+\mathbf{Q}_l+\mathbf{Q}_m=0} \int_{\mathbf{q}_1+\mathbf{q}_2+\mathbf{q}_3+\mathbf{q}_4=0} \gamma_4 A_i(\mathbf{q}_1)A_j(\mathbf{q}_2)A_l(\mathbf{q}_3)A_m(\mathbf{q}_4) \tag{19}$$

where $\int_q \equiv 1/(2\pi)^3 \int d^3q$, and $A(\mathbf{q}) \equiv A(\mathbf{r})e^{-i\mathbf{q}\mathbf{r}}\, d^3r$. The vertex functions γ_3, γ_4 do depend on q_1, q_2, ... However this dependence can be neglected since typical values $q \sim q_1 \sim q_2 \ldots \sim 1/\xi$ are much smaller than $q^* \sim 1/R_n$, where ξ is the interfacial thickness, $\xi \gg R_n = n^{1/2}a$ (this inequality is verified below). Neglecting also a weak dependence of γ_4 on a subset $\{ijkl\}$ of basic vectors (this is a standard approximation[35,36]), and taking into account that $\gamma_2(q^* + q) \simeq \tau + Cq^2$, we get the free energy per unit interfacial area

$$F = \int dz \left\{ f(\mathbf{A}) + \frac{1}{2}C\sum_i \mu_i \left|\frac{dA_i}{dz}\right|^2 \right\} \tag{20}$$

where $\mu_i = \cos^2\theta_i$, θ_i is the angle between Q_i and the normal to the interface, $\mathbf{A} = \{A_i(z)\}$, and

$$f(\mathbf{A}) = \frac{\tau}{2}\sum_i |A_i|^2 + \frac{\gamma_3}{3!}\sum_{\mathbf{Q}_i+\mathbf{Q}_j+\mathbf{Q}_l=0} A_iA_jA_l + \frac{\gamma_4}{4!}\sum_{\mathbf{Q}_i+\mathbf{Q}_j+\mathbf{Q}_l+\mathbf{Q}_m=0} A_iA_jA_lA_m \tag{21}$$

Note that

$$A_i = A_j^* \quad \text{if} \quad \mathbf{Q}_i + \mathbf{Q}_j = 0 \tag{22}$$

Coexistence of disordered and bcc morphologies implies that the function $f(\mathbf{A})$ must show equal minima at $A_i = 0$ and $A_i = A_0$. These requirements specify the transition "temperature"

$$\tau^* = \frac{16}{135}\frac{\gamma_3^2}{\gamma_4} \tag{23}$$

and the amplitude

$$A_0 = -\frac{8}{45}\frac{\gamma_3}{\gamma_4} \tag{24}$$

as obtained in refs 3 and 13. Introducing reduced

variables $\tilde{A}_i = A_i/A_0$, and $\tilde{z} = z/\xi$, we rewrite eq 20 for $\tau = \tau^*$:

$$F = \sigma_0 \tilde{F}, \qquad \sigma_0 = \frac{1}{3}\frac{2^9}{45^3}\frac{{\gamma_3}^4}{{\gamma_4}^3}\xi, \qquad \xi = \frac{3}{4}\frac{\sqrt{15\gamma_4 C}}{\gamma_3} \quad (25)$$

$$\tilde{F} = \int d\tilde{z}\left\{\tilde{f}(\tilde{\mathbf{A}}) + \sum_i \mu_i \left|\frac{d\tilde{A}_i}{d\tilde{z}}\right|^2\right\} \quad (26)$$

where

$$\tilde{f}(\tilde{\mathbf{A}}) = \sum_i |\tilde{A}_i|^2 + \frac{1}{4}\sum_{\mathbf{Q}_i+\mathbf{Q}_j+\mathbf{Q}_l=0} \tilde{A}_i\tilde{A}_j\tilde{A}_l + \frac{1}{45}\sum_{\mathbf{Q}_i+\mathbf{Q}_j+\mathbf{Q}_l+\mathbf{Q}_m=0} \tilde{A}_i\tilde{A}_j\tilde{A}_l\tilde{A}_m$$

The interfacial tension, $\sigma = \sigma_0 \min \tilde{F}$, depends on the orientation of the interface with respect to the basic wavevectors of bcc structure. The dependence comes from the coefficients $\mu_i = \cos^2 \theta_i$ (see eq 26). A sort of averaged interfacial tension, σ_{av}, can be obtained by substituting μ_i in eq 26 by their averaged (over all orientations) values $\langle\mu_i\rangle = 1/3$ (in fact thus defined σ_{av} must exceed σ averaged over all orientations of the interface). A simplification then comes from the fact that (with $\mu_i = 1/3$) the functional $\tilde{F}$ becomes symmetric with respect to a transposition of the amplitude set $\{A_i\}$ since all basic wavevectors are now equivalent. Hence it is reasonable to assume that all amplitudes must be equal: $A_i(z) = A(z)$; we can also assume that A is real (see eq 22). Then eq 26 can be rewritten as

$$\tilde{F} = \int d\tilde{z}\left\{12\tilde{A}^2(1-\tilde{A})^2 + 4\left|\frac{d\tilde{A}}{d\tilde{z}}\right|^2\right\}$$

Minimization of the above functional yields

$$\sigma_{av} = \sigma_0 \min \tilde{F} = \frac{4}{\sqrt{3}}\sigma_0 \quad (27)$$

The interfacial thickness is $\xi \sim R_n/\epsilon$ (see eq 25), i.e., $\xi \gg R_n$ as assumed above.

Next let us calculate $\sigma = \sigma_m$ for the interface which is parallel to six basic wavevectors: Q_i, $i = 1-6$ (i.e., parallel to one of the edges of the corresponding tetrahedron). Then $\mu_i = 0$ for $i = 1-6$, and $\mu_i = 2/3$ for $i = 7-12$. This orientation is expected to be favorable precisely because the gradient term (the second term in curly brackets in the right-hand side of eq 26) vanishes for half of the amplitudes. With two subsets of equivalent wavevectors (Q_i with $i = 1-6$ and $i = 7-12$) we have to allow two different amplitudes: $A_i = A$ for $i = 7-12$ and $A_i = B$ for $i = 1-6$. The reduced interfacial energy is

$$\tilde{F} = \int d\tilde{z}\left\{6(\tilde{A}^2+\tilde{B}^2) - 6\tilde{B}(3\tilde{A}^2+\tilde{B}^2) + 8\tilde{A}^2\tilde{B}^2 + 2(\tilde{A}^4+\tilde{B}^4) + 4\left|\frac{d\tilde{A}}{d\tilde{z}}\right|^2\right\}$$

Minimizing it with respect to $\tilde{A}(\tilde{z})$ and $\tilde{B}(\tilde{z})$ we get $\tilde{F} \simeq 0.92(4/3^{1/2})$, i.e., $\sigma_m \simeq 0.92\sigma_{av}$. Taking into account that σ_m is expected to be the lowest value of the interfacial tension and that σ_{av} is (perhaps slightly) higher than the *average* tension, we conclude that the variation of σ (as a function of the orientation) does not exceed 8%; i.e., orientation dependence of σ is weak and can be neglected. Hence we will use the constant interfacial tension approximation for the dis/bcc transition: $\sigma = \sigma_{av}$. Using approximate values of the vertex factors calculated for regular multiblock copolymers:[13,37]

$$\gamma_4 \simeq 129; \qquad \gamma_3 \simeq 110\epsilon; \qquad C \simeq 9.06{R_n}^2 \quad (28)$$

we get the dis/bcc interfacial tension (in k_BT/nv units):

$$\sigma \simeq \sigma_{av} \simeq 0.27 R_n \epsilon^3 \quad (29)$$

Let us turn to the cyl/lam morphological transition. Here the interfacial tension strongly depends on the mutual orientation of lamellar sheets, "cylinders", and the interface. If the interface is parallel to both cylinders and lamellae, then the interfacial structure can be treated in analogy with the dis/bcc case (see eq 20). The result is also similar:

$$\sigma_{||} \sim R_n \epsilon^3 \quad (30)$$

It is clear from eq 20 that the lowest tension can be achieved with the lowest μ_i. Hence let us consider a different orientation of the interface tilted to both lamellae and cylinders by the angle $\pi/2 - \theta$. Obviously the tilt can be taken into account by renormalization of the prefactors in the gradient term: $\mu_i \rightarrow \mu_i \cos^2(\pi/2 - \theta)$. Using the approach described above it is easy to show that the surface tension then changes as:

$$\sigma(\theta) \simeq \sigma_{||} \sin\theta \quad (31)$$

if θ is not too small.

Obviously all $\mu_i = 0$ if the interface is perpendicular to both lamellae and cylinders, i.e., $\theta = 0$. In this case eq 20 can no longer be applied (its minimization results in vanishing interfacial energy), so we have to take into account higher-order gradient terms following ref 36. The result is

$$F = \int dz\left\{f(\mathbf{A}) + \frac{1}{8}C(q^*)^{-2}\sum_i \left|\frac{d^2A_i}{dz^2}\right|^2\right\} \quad (32)$$

where $f(A)$ is still defined in eq 21 with the appropriate set Q_i. For 2d hexagonal (cylindrical) morphology the set must consist of three vectors forming a perfect triangle plus three antiparallel vectors. It it natural to assume that the lowest tension corresponds to the situation when lamellar and cylindrical structures are "epitaxially related", i.e., that the basic wavevectors $\{Q, -Q\}$ of the lamellar structure belong to the cylindrical set (that is, lamellae are parallel to a plane connecting nearest neighboring cylinders), so that the whole cyl/lam structure is also determined by the same set of six vectors corresponding to 2d hexagonal symmetry.

The free energy, eq 32, can be minimized with a procedure analogous to that used above for dis/bcc interfaces. The result is (note that $q^* \sim 1/R_n$)

$$\sigma_\perp \sim R_n \epsilon^{3.5} \quad (33)$$

Thus $\sigma_\perp/\sigma_{||} \sim \epsilon^{1/2} \ll 1$, i.e., perpendicular orientation of

the interface is strongly preferred (a similar conclusion had been drawn for the dis/lam interface[36]).

4. Secondary Structures for the dis → bcc Transition

4.1. The Stability Window. In the previous sections we set up the general free energy expressions in terms of two order parameter fields: $\psi(r)$ related to composition and $\varphi(r)$ related to the block length. In the case of weak polydispersity the spatial pattern $\psi(r)$ is nearly the same as for the reference monodisperse system with the same primary morphology, so that we just need to specify which morphology in which (secondary) domain instead of specifying the whole field $\psi(r)$. In particular in the transition regime from disordered to ordered (bcc) primary structure we expect coexistence of both morphologies, so that the global structure can be defined by the function $\Theta(r) = 0$ in the disordered regions and $\Theta(r) = 1$ in the bcc regions. Then the field $h(r)$ defined in eq 9 in terms of $\psi(r)$ is

$$h(r) = h_{bcc}\Theta(r) \tag{34}$$

where h_{bcc} is a constant depending on the average composition asymmetry. Using eqs 9, 18, 24, and 28 we get

$$h_{bcc} = 12A_0^2X^* \simeq 2.86\gamma_3^2/\gamma_4^2 \simeq 2.08\epsilon^2 \tag{35}$$

(note that $X^* \simeq 7.55$).

The equilibrium second-order parameter field $\varphi(r)$ must correspond to the minimum of the total free energy, eq 17. As verified below, the φ-dependence of the nonlocal and interfacial parts of the free energy is negligible: the dominant φ-dependence comes from the local term. Minimizing $F_{local} = \int f_{local}\, d^3r$ (here f_{local} is defined in eq 14) over φ under the condition of fixed gross molecular weight distribution of blocks, eq 7, we get

$$\varphi(r) = (h(r) - ph_{bcc})/\kappa \tag{36}$$

where p is the fraction of the total volume occupied by the bcc morphology. Using eqs 14, 36, and 34 we get

$$F_{local}/V = -\frac{1}{2\kappa}p(1-p)h_{bcc}^2 + pf_{bcc} \tag{37}$$

where $f_{bcc} = f_1^{(0)}(\tau)$ is the free energy density for the bcc morphology of the reference regular block-copolymer system; we take into account that in the disordered state $f_1 = 0$ by definition.

Then we minimize the local free energy (again contributions of other free energy terms are negligible) with respect to p to obtain

$$p = 0.5 - \kappa f_{bcc}/h_{bcc}^2 \tag{38}$$

Next we take into account that $f_{bcc} = f_{dis} = 0$ at the dis/bcc transition point $\tau = \tau^*$ (see eq 23). Equation 3 implies that $\partial f_1^{(0)}/\partial\tau = (1/2)\langle\psi^2\rangle_{local}$, that is $f_{bcc} \simeq (1/2)(h_{bcc}/X^*)(\tau - \tau^*)$ if τ is close enough to the transition point: $|\tau - \tau^*| \ll \epsilon^2$, where ϵ^2 is the characteristic scale for τ. Then we rewrite eqs 37 and 38 as

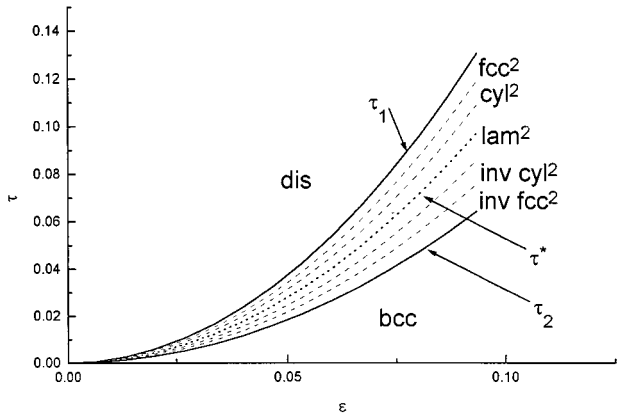

Figure 3. Phase diagram of a weakly polydisperse ($\delta = 0.2$) multiblock copolymer near the transition line $\tau = \tau^*$ (dotted line) between disordered state and bcc primary morphology. Secondary structures are stable in the region between the solid lines. Dashed lines correspond to transitions between different secondary morphologies.

$$F_{local}/V = -\frac{1}{2\delta}\left(\Delta - \frac{h_{bcc}\delta}{2}\right)^2$$

$$p = 0.5 - \frac{1}{h_{bcc}\delta}\Delta \tag{39}$$

where $\Delta \equiv (\tau - \tau^*)/2X^* \simeq (\chi^* - \chi)/\chi^*$ is the relative distance to the dis/bcc transition at $\chi = \chi^*$. Obviously the interesting Δ range is $|\Delta| \sim h_{bcc}/\kappa \sim \epsilon^2\delta$, i.e., $|\tau - \tau^*| \sim \epsilon\delta \ll \epsilon^2$ as assumed above.

Thus the weaker the polydispersity, the stronger the dependence of the volume fraction of bcc domains, p, on Δ, i.e., on the interaction parameter. The same conclusion also applies to the equilibrium secondary domain size Λ which depends on p as shown below.

Using eq 35 we rewrite the second equation (39) as

$$\tau = \tau^*[1 + 1.4\delta(1 - 2p)]$$

where $\tau^* = (16/135)(\gamma_3^2/\gamma_4) \simeq 11.2\epsilon^2$ is defined in eq 23. The system thus forms secondary superstructures in a narrow window around the dis/bcc transition line $\tau^* \simeq 11.2\epsilon^2$: $\tau_1 > \tau > \tau_2$, where $\tau_1 = \tau^*(1 + 1.4\delta)$ corresponds to $p = 0$, i.e., the onset of nucleation of bcc domains in the disordered matrix, and $\tau_2 = \tau^*(1 - 1.4\delta)$ corresponds to $p = 1$, i.e., to the onset of nucleation of disordered domains in bcc matrix (see Figure 3).

4.2. Scaling Estimates. The local free energy as defined in eqs 37 and 38 does not depend either on the secondary domains size Λ or on their shape. Therefore the secondary structure is determined by the last two free energy terms (see eq 17): nonlocal free energy and the energy of secondary interfaces. In fact the nonlocal energy, eq 15, increases as the domain size is increased; on the other hand the total interfacial area, and hence interfacial energy, is smaller with larger domains. The equilibrium Λ is a compromise between these opposite tendencies.

Equation 36 can be rewritten as $\varphi = h^*\tilde{\varphi}/\kappa$, where $h^* \equiv h_{bcc}$ and

$$\tilde{\varphi}(r) = \begin{cases} 1 - p, & \text{bcc} \\ -p, & \text{dis} \end{cases} \tag{40}$$

Assuming a *periodic* secondary structure, i.e., periodic $\varphi(r)$ with the typical scale Λ, we estimate the nonlocal free energy, eq 15, as

$$F_{\text{nloc}} \sim \frac{\kappa^2}{V^3 n a^2} \frac{V^4 \varphi^4}{(1/\Lambda)^2} \sim V \frac{\Lambda^2}{R_n^2} \delta^2 h^{*4}$$

where we assumed that the typical $\varphi_q \sim V h^* \delta$ and that the sum in eq 15 is dominated by a few first terms. An analogous estimate for F_{intf} (within the constant interfacial tension approximation) is

$$F_{\text{intf}} \sim V\sigma/\Lambda$$

Obviously the total excess free energy

$$F_{\text{ex}} = F_{\text{nloc}} + F_{\text{intf}}$$

attains a minimum (the local free energy is constant once p is determined and thus it is irrelevant here) when both contributions are of the same order, i.e.

$$\Lambda \sim \Lambda_0 \equiv \left(\frac{\sigma R_n^2}{\delta^2 h^{*4}}\right)^{1/3}$$

$$F_{\text{ex}}/V \sim E_0 \equiv \left(\frac{\sigma \delta h^{*2}}{R_n}\right)^{2/3} \tag{41}$$

Note that nonlocal free energy per unit volume is thus of order $E_0 = (\sigma \delta h^{*2}/R_n)^{2/3} \sim \epsilon^{14/3} \delta^{2/3}$ since $\sigma \sim R_n \epsilon^3$ and $h^* = h_{\text{bcc}} \sim \epsilon^2$. Therefore $E_0 \ll |F_{\text{local}}|/V \sim h^{*2}/\kappa$ if

$$\epsilon^2 \ll \delta \tag{42}$$

One can easily check that this condition coincides with the condition (16) of validity of eq 15. Condition 42 corresponds to the so-called true weak segregation limit considered in ref 27; it is assumed below. Hence (in the regime defined by condition 42) the nonlocal free energy is indeed negligible in comparison with the local term, as was assumed in the previous section.

The typical secondary domain size as defined above scales as

$$\Lambda_0 \sim R_n \epsilon^{-5/3} \delta^{-2/3} \tag{43}$$

(this estimate was originally obtained in ref 27). Note that Λ_0 is much larger than both the block size R_n and the interfacial thickness ξ. Therefore secondary domains are well developed, i.e., secondary superstructures should be qualified as *strong*.

4.3. The Phase Diagram. To quantitatively analyze the secondary structures it is convenient to introduced the reduced quantities: $F = F_{\text{ex}}/(E_0 V)$, $\tilde{r} = r/\Lambda_0$, and $\tilde{\varphi} = \kappa\varphi/h^*$, so that $\varphi(r) = h^* \tilde{\varphi}(r/\Lambda_0)/\kappa$ and

$$F = \frac{1}{2\tilde{V}^4} \sum_{\tilde{q},\tilde{q}'} \frac{|\tilde{\varphi}_{\tilde{q}}|^2 \, |\tilde{\varphi}_{\tilde{q}'}|^2}{\tilde{q}^2 + \tilde{q}'^2} + \frac{\tilde{A}}{\tilde{V}} \tag{44}$$

where "tilde" indicates the reduced variables; $\tilde{V} = V/\Lambda_0^3$ is the reduced volume, and $\tilde{A} = A/\Lambda_0^2$ is the reduced interfacial area. Obviously

$$\min_{\tilde{\varphi}} F$$

depends only on p: F does not depend on the volume $\tilde{V}$ since both $\tilde{\varphi}_{\tilde{q}} \equiv \int \tilde{\varphi}(r) \exp(i\tilde{q}\tilde{r}) \, d^3\tilde{r}$ and $\tilde{A}$ are proportional to the volume (remember that $\tilde{\varphi}$ is assumed to be a periodic function of $\tilde{r}$ which takes two values as defined in eq 40). The "tilde" attribute is omitted from now on, i.e., length and the order parameter φ are reduced with Λ_0 and $h^*\delta$ correspondingly.

The volume fraction of bcc domains, p, is thus determined by the local free energy (see eqs 39), whereas the secondary domain size Λ, the secondary morphology, and the excess free energy (on top of the local free energy) can be determined by minimization of F with respect to φ at a fixed p. The functional F is invariant with respect to simultaneous transformations $\varphi \to -\varphi$, $p \to 1 - p$ which physically correspond to the inversion of the (secondary) morphology, i.e., replacement of bcc domains by disordered and vice versa. Hence we only have to consider the regime $p < 1/2$: equilibrium morphologies for $p > 1/2$ can be easily generated by the inversion.

The simplest *lamellar* secondary morphology expected for $p \simeq 1/2$ implies alternating bcc and disordered sheets of thickness $p\Lambda$ and $(1 - p)\Lambda$ correspondingly (see Figure 4). The free energy, eq 44, is calculated in Appendix A

$$F = K_1(p)\Lambda_2 + \frac{2}{\Lambda} \tag{45}$$

where

$$K_1(p) = \frac{1}{24} p^3 (1-p)^3 - \frac{1}{4\pi^5} \sum_{s=1}^{\infty} \frac{\sin^2(\pi p s)}{s^5} \frac{\sinh(\pi(1-p)s) \sinh(\pi p s)}{\sinh(\pi s)}$$

Minimizing F over Λ we get

$$\Lambda = [K_1(p)]^{-1/3}; \qquad F = 3[K_1(p)]^{1/3} \tag{46}$$

The dependence of the reduced period Λ on p is shown in Figure 6a. Note a minimum at $p = 1/2$ and a strong increase of Λ as p tends to 0 (or to 1). In the regime $p \ll 1$ the last equation can be rewritten as (see eq A6)

$$F \simeq \frac{3}{(4\pi)^{1/3}} p^{4/3} \left(\ln \frac{1}{p} - 1.55\right)^{1/3} \tag{47}$$

Let us consider other than lamellar secondary morphologies. In the regime $p \ll 1$, i.e., low volume fraction of ordered component, we expect nearly *spherical* bcc domains arranged in a 3d periodic structure. The following most common superstructures have been analyzed: simple cubic (cubic), body centered cubic (bcc), face centered cubic (fcc), hexagonal closed packed (hcp). Let R be the radius of a spherical bcc domain. The free energy can be written as

$$F = K_3(p)R^2 + \frac{3p}{R}$$

where two terms on the right-hand side correspond to nonlocal and interfacial energies. The nonlocal factor $K_3(p)$ is calculated in Appendix B. The result is

$$K_3(p) \simeq p^2\{0.04374 - 0.4p + sp^{4/3}\} \tag{48}$$

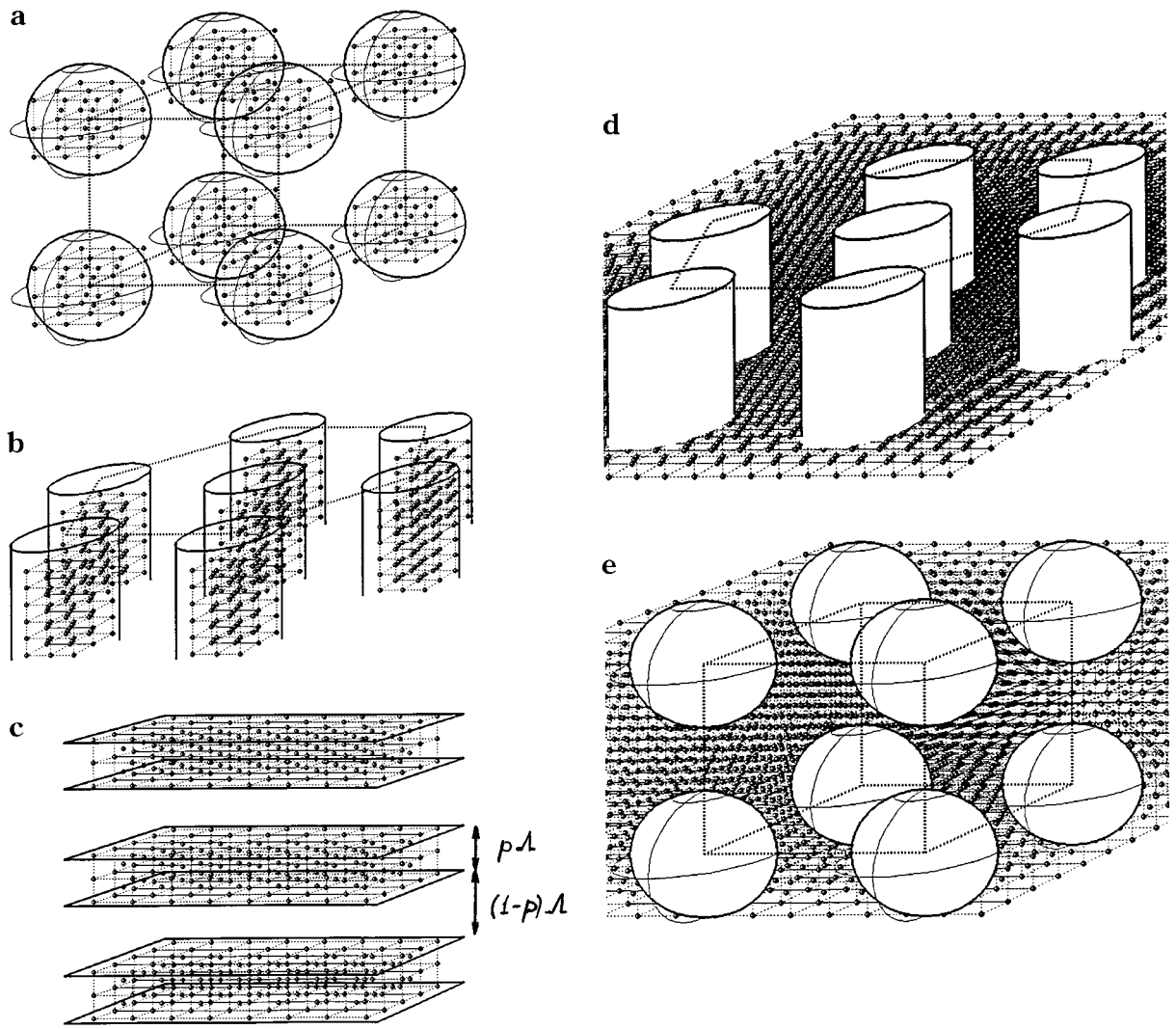

Figure 4. Secondary structures predicted near the dis/bcc transition line: (a) fcc array of bcc spherical domains in disordered matrix; (b) hexagonal array of bcc cylinders in disordered matrix; (c) alternating ordered (bcc) and disordered lamellar sheets; (d) disordered cylinders in bcc matrix; (e) disordered secondary spheres in bcc matrix. Note that simple cubic arrangements are shown for simplicity instead of bcc.

where s = 0.475 478 79 (cubic), 0.471 083 41 (bcc), 0.470 926 95 (hcp), and 0.470 926 26 (fcc). Thus it is the fcc secondary structure that corresponds to the lowest free energy. Note however that the energy difference between fcc and hcp structures is extremely small. Minimizing F over R we get

$$R = \left(\frac{3p}{2K_3(p)}\right)^{1/3}; \qquad F = 3(9p^2K_3(p)/4)^{1/3} \tag{49}$$

An analogous consideration of *cylindrical* secondary structures (again assuming that $p \ll 1$) results in $F = K_2(p)R^2 + (2p/R)$, where

$$K_2(p) = 0.11351p^2 + 0.25p^3 \ln p + s'p^3 \tag{50}$$

with $s' = 0.02345$ for square lattice of cylinders, and $s' = 0.02224$ for hexagonal lattice which is therefore more favorable. The free energy obtained after minimization over R is

$$F = 3(p^2K_2(p))^{1/3} \tag{51}$$

Comparing the free energies given by eqs 47, 51, and 49 for three secondary morphologies, we find that spherical morphology wins for low p. We also expect that the cylindrical (hexagonal) morphology must be stable in some intermediate p-range. To locate the corresponding morphological transitions, we calculated the free energy numerically minimizing F, eq 44, with respect to the size and shape of the secondary domains (the asymptotic expressions, eqs 48 and 50, are not useful here as they are valid only in the limit $p \ll 1$). The numerical analysis confirms the analytical results considered above. The calculated free energies of different structures are compared in Figure 5. Note that free energies of bcc, fcc, and hcp structures are indistinguishable in the scale of this figure. We found the following equilibrium secondary morphologies: fcc array of spheres (spheres are characterized by bcc primary structure and the matrix is disordered, Figure 4a) for $0 < p < 0.174$; hexagonal array of cylinders for $0.174 < p < 0.323$ (Figure 4b); lamellar structure for $0.323 < p < 1 - 0.323$ (Figure 4c); and inverse cylindrical and inverse spherical superstructures for $0.677 < p < 0.826$ and $0.826 < p < 1$ correspondingly (see Figure 4d,e). The numerical study also shows that simple cubic and bcc arrangements of secondary spherical domains are less favorable than a fcc structure. However it was not possible to discriminate numerically between fcc and

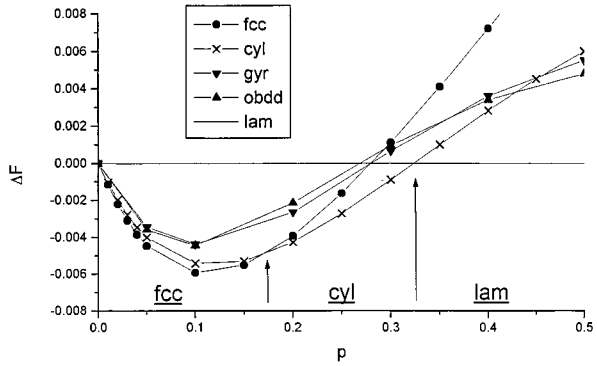

Figure 5. The calculated excess free energies ΔF of face centered cubic spherical (fcc), cylindrical (cyl), gyroid (gyr), and ordered bicontinuous double diamond (obdd) secondary morphologies as a function of volume fraction p of the ordered domains, $\Delta F = F - F_{lam}$.

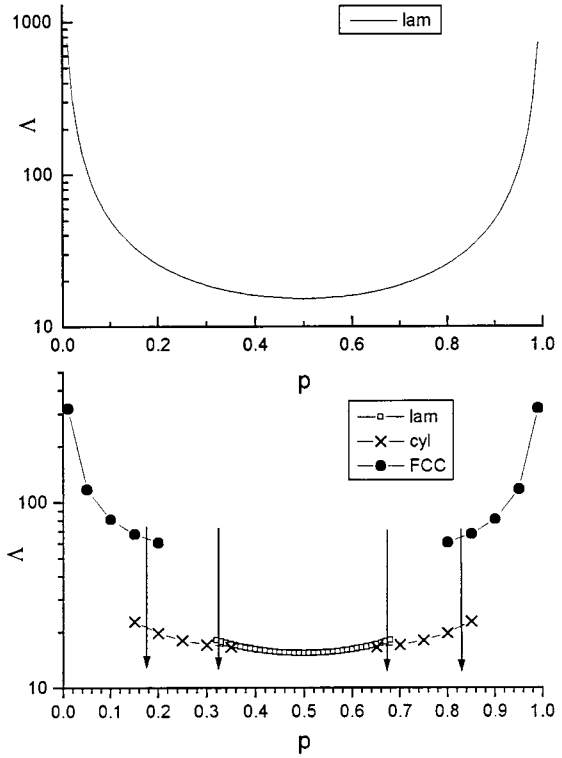

Figure 6. The dependence of the reduced period Λ of secondary structures on volume fraction p of ordered domains (i.e., domains characterized by bcc primary morphology): (a) for lamellar secondary structure; (b) for all secondary structures predicted near the dis/bcc transition line.

hcp superstructures: the free energy difference is too small in comparison with the numerical error.

Bicontinuous secondary structures (gyroid and double diamond) have been also analyzed numerically. However we found that they are never truly stable: at any p the lowest free energy is attained with one of other structures considered above.

The dependence of the (reduced) period of a secondary structure, Λ, on p is shown in Figure 6b. In general we define Λ as $2\pi/Q$, where Q is the basic (i.e., the lowest) wavenumber of the secondary structure; $\Lambda = (16\pi/3^{5/2})^{1/3}Rp^{-1/3}$ for spherical fcc morphology, and $\Lambda = (3^{1/2}\pi/2)^{1/2}Rp^{-1/2}$ for cylindrical hexagonal morphology. Note a noticeable discontinuity of Λ at the hex/fcc transition, and also a strong increase of the period in the regimes of spherical morphology (p close to 0 and to 1). Hence the secondary domain size is very sensitive to variation of external parameters such as χ: a really small change of the interaction parameter by $\Delta\chi/\chi^* \sim \epsilon^2\delta$ could result in a variation of the equilibrium domain size by a factor of 2 or more.

5. Secondary Structures for the cyl → lam Transition

5.1. The Stability Window. Secondary superstructures must be also stable near the transition line between cylindrical and lamellar primary morphologies. The window of their stability is determined by the local free energy term (and eventually by the polydispersity degree) in complete analogy with the dis/bcc transition considered above. Using eqs 7 and 14 the local free energy can be written as

$$F_{local} = V(h_{cyl}\Delta + f^*) + \int\left[(h(r) - h_{cyl})(\Delta - \varphi(r)) + \frac{1}{2}\kappa\varphi^2(r)\right] d^3r$$

Here we use the approximation $f_1^{(0)} \simeq f^* + h\Delta$, where f^* is the free energy density at the transition point $\tau = \tau^*$ for the reference regular block-copolymer system and $\Delta = (\tau - \tau^*)/2X$ (note that in this section τ^* corresponds to the cyl/lam transition, $\tau^* \simeq -2.87\gamma_3^2/\gamma_4 \simeq -269.2\epsilon^2$ as can be deduced from the weak segregation theories[3,13]). The function $h(r)$ takes two values: h_{cyl} in the regions with cylindrical primary morphology and h_{lam} otherwise (i.e., in lamellar regions).

Volume fraction p of lamellar regions is related to τ in the same way as for dis/bcc transition (see the second eq 39) with h_{bcc} replaced by $h^* = h_{lam} - h_{cyl}$:

$$\tau = \tau^* + (h_{lam} - h_{cyl})X^*(1 - 2p)\delta$$

Taking into account that $h_{lam} = 2A_{lam}^2X^* \simeq 86.67\gamma_3^2/\gamma_4^2$ and $h_{cyl} = 6A_{cyl}^2X^* \simeq 75.38\gamma_3^2/\gamma_4^2$

$$h^* \simeq 8.2\epsilon^2 \qquad (52)$$

(here A_{lam} and A_{cyl} are the amplitudes of the corresponding primary structures defined in analogy with A_0 for the bcc structure) we get $\tau \simeq \epsilon^2(-269.2 + 62\delta(1 - 2p))$, i.e., the secondary structures are stable in the range $\tau_1 > \tau > \tau_2$, where $\tau_1 \simeq \epsilon^2(-269.2 + 62\delta)$ and $\tau_2 \simeq \epsilon^2(-269.2 - 62\delta)$.

5.2. Secondary Morphologies. The secondary structure is determined by the function

$$\tilde{\varphi}(r) = \begin{cases} 1 - p, & \text{lam} \\ -p, & \text{cyl} \end{cases}$$

defined in analogy with eq 40. The second-order parameter $\varphi(r)$ and the nonlocal free energy can be defined in terms of $\tilde{\varphi}$ in exactly the same way as considered in section 4. The only difference is that the parameter $h^* = h_{bcc}$ must be replaced by $h^* = h_{lam} - h_{cyl}$. In particular $\varphi(r) = h^*\tilde{\varphi}(r)/\kappa$.

The shape of secondary domains is determined by the competition between the nonlocal and interfacial free energy. The nonlocal energy does not depend on the orientation of primary lamellae and cylinders with respect to secondary domains. However the interfacial energy does depend on the orientation: it strongly favors the situation when both lamellae and cylinders are perpendicular to the interfaces (see section 3). This implies that all interfaces must be parallel, i.e., lamellar

superstructure. The secondary period Λ can be calculated in the same way as for the dis/bcc case: its characteristic value Λ_0 is defined in eq 41 and its p-dependence is given by the factor $K_1(p)^{-1/3}$ (see eq 46):

$$\Lambda = \Lambda_0[K_1(p)]^{-1/3}$$

However one must substitute the appropriate interfacial tension $\sigma = \sigma_\perp$, eq 33, and h^*, eq 52, in eq 41. The result is

$$\Lambda_0 = \left(\frac{\sigma_\perp R_n^{\,2}}{\delta^2 h^{*4}}\right)^{1/3} \sim R_n \epsilon^{-3/2}\delta^{-2/3} \qquad (53)$$

Note that the secondary period for the cyl/lam transition is shorter than that for the dis/bcc case (see eq 43) by a factor of order $\epsilon^{1/6}$.

Secondary structures other than lamellar (cylindrical, spherical) are strongly suppressed in the cyl/lam window since these structures imply that some parts of the secondary interfaces must be nearly parallel to lamellae or cylinders invoking much higher interfacial tension $\sigma_\parallel \gg \sigma_\perp$ (see eqs 30 and 33). Hence we expect a wide region of lamellar secondary structure nearly covering the whole window $\tau_1 < \tau < \tau_2$. However in the case of high asymmetry $p \ll 1$ (or $1 - p \ll 1$), i.e., close to τ_1 (or τ_2), nonlamellar structures become competitive because of their lower nonlocal energy. In is natural to assume that minor lamellar sheets are replaced by disklike objects arranged in a superlattice at low p. The interfacial energy per disk of thickness $2R$ and diameter D is

$$F_{\text{intf}} = 2A_{\text{base}}\sigma_\perp + A_{\text{side}}\sigma_\parallel \qquad (54)$$

where $A_{\text{base}} = \pi D^2/4$ is the base area of the disk, and $A_{\text{side}} = 2\pi RD$ is its side surface area. (Note that we do not actually have to assume cylindrical shape of the side surface: for a disk with rounded edge the contribution of the side surface is still $2\pi RD\sigma_\parallel$ as can be obtained by integration of the interfacial tension $\sigma = \sigma(\theta)$, where θ is the angle between the local normal to the surface and normal to the base, over the side surface area taking into account that $\sigma(\theta) \simeq \sigma_\parallel \sin\theta$ if θ is not too small, see eq 31.) The reduced interfacial energy per unit volume expressed in units of

$$E_0 = \left(\frac{\sigma_\perp \delta h^{*2}}{R_n}\right)^{2/3}$$

is

$$F_{\text{intf}} = \frac{F_{\text{intf}}}{(V_{\text{disk}}/p)E_0} = p\left(\frac{1}{R} + \frac{4\lambda}{D}\right)$$

where $V_{\text{disk}} \simeq 2RA_{\text{base}}$, $\lambda \equiv \sigma_\parallel/\sigma_\perp \sim \epsilon^{-1/2}$, and both sizes R and D are reduced, i.e., expressed in Λ_0 units.

The nonlocal free energy calculated in the logarithmic approximation is

$$F_{\text{nloc}} \simeq \frac{1}{\pi} R^2 p^2 \ln\alpha$$

where $\alpha \equiv D/R$. Minimizing the total reduced excess free energy per unit volume

$$F = F_{\text{nloc}} + F_{\text{intf}}$$

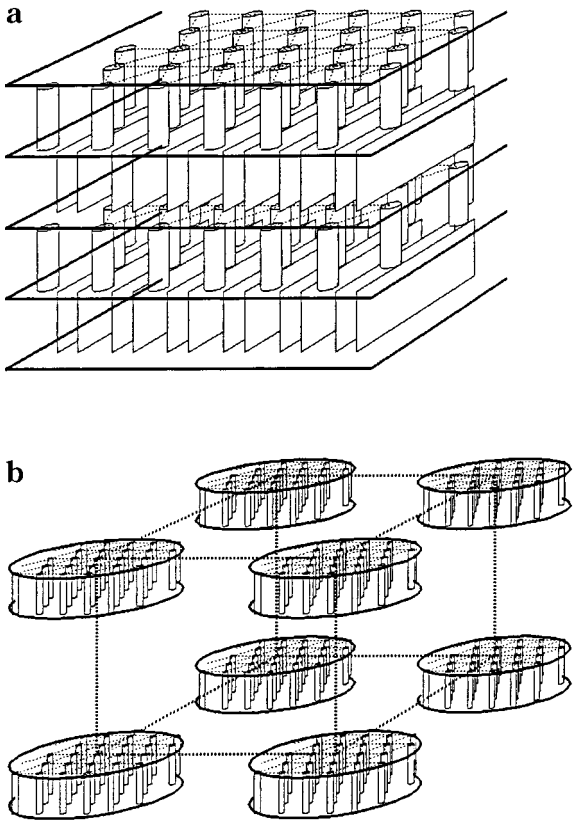

Figure 7. Secondary structures near the cyl/lam transition line: (a) lamellar sheets; (b) asymmetric disks arranged in an fcc superlattice (the disks are perforated by primary cylinders). Not all the disks are shown.

with respect to R and D we get

$$F \simeq \frac{3}{(4\pi)^{1/3}}(p^4 \ln\alpha)^{1/3}; \qquad R \simeq \left(\frac{\pi}{2p\ln\alpha}\right)^{1/3} \qquad (55)$$

where $\alpha = D/R$ is defined by the equation $\alpha/\ln\alpha \simeq 8\lambda$; the approximate solution is $\alpha \simeq 8\lambda \ln\lambda$. Comparing the free energy of the disk structure, eq 55, and that of lamellar structure, eq 47, we locate the transition between the two secondary structures at

$$p_t \sim 1/\alpha \sim 1/(\lambda \ln\lambda)$$

i.e., p_t is small. The period Λ of the lamellar secondary structure at the transition point is of the order of the disk diameter

$$\Lambda \sim D \sim p_t^{-4/3}\left(\ln\frac{1}{p_t}\right)^{-1/3}$$

Omitting logarithmic factors we thus get $\Lambda \sim \epsilon^{-2/3}$ in Λ_0 units.

The lamellar secondary superstructure (see Figure 7a) is stable in the wide range $p_t < p < 1 - p_t$. For $p < p_t$ the equilibrium secondary morphology is comprised of disklike domains "perforated" by primary cylinders (Figure 7b) in the matrix characterized by primary lamellar structure (not shown in the figure). The disks are arranged in the fcc superlattice (the superlattice symmetry is determined by the structural contributions F_{11} and F_{21} to the free energy which are insensitive to the domain shape, see Appendix B). For $p > 1 - p_t$ we

predict a similar secondary morphology, but with disks "perforated" by primary lamellae in the "cylindrical" matrix.

So far we assumed that interfacial tension at the side disk surface is constant ($=\sigma_{||}$). This is not exactly the case however: parts of the side surface that are perpendicular to lamellae are characterized by lower tension than those parallel (yet the scaling estimate, eq 30, applies to both situations). As a result the equilibrium shape of the disks must be noncircular: the disks are prolate perpendicular to primary lamellar sheets. However this shape change does not affect any of the scaling results obtained above.

The disklike domain shape is a result of incompatibility of the favorable perpendicular orientation of primary domains (say, lamellar sheets) at the surface of secondary domains and their spherical shape. This incompatibility is true provided that the primary structure is not distorted (free of defects). With defects the perpendicular boundary condition can be essentially fulfilled even for spherical domains[36,38] (lamellar or smectic structures have been considered in this regard). Also the energetic cost of smectic defects might be not high thus favoring nearly spherical domains with distorted primary structure. However the defect-free (nonspherical) domains are still favorable provided that their size is not too large.[36,38] This implies that the above results are valid if the polydispersity degree is not too low, as the secondary domain size is inversely proportional to δ (see eq 53). Using the results obtained in ref 38, we managed to get a more precise condition: the defects are not important in the regime $p(1-p) \geq p_t$ if

$$\delta \gg \epsilon^{(3/4)((3-n)/(2-n))-1} \sim \epsilon^{0.875} \qquad (56)$$

where $n \simeq 4/3$ is the Apollonius scaling index.[39] This condition (56) is stronger than condition 42 assumed above. We do not intend to discuss here the delicate intermediate regime $\epsilon^2 \ll \delta \ll \epsilon^{0.875}$ where distorted primary structures with defects might be relevant.

6. Discussion and Conclusions

We investigate domain structures that can be formed in multiblock copolymers with some polydispersity of molecular weights of the blocks. Unusual secondary superstructures that form on top of normal (primary) domain structures characteristic for block copolymers are predicted in some windows near morphological transitions between different primary structures. These windows essentially replace biphasic regions of macroscopic separation between different domain structures predicted for polydisperse *di*block copolymers.[9,11] The driving force for formation of secondary domain structures is generic for all macromolecules with quenched disorder of monomer sequence: it comes from competition between the fractionation effect of a first-order morphological transition and chemical connectivity of chain fragments with different composition and/or different primary structure. Therefore secondary domain structures are expected both for weakly polydisperse multiblock copolymers and for completely random block copolymers (the latter case will be considered separately).

The quantitative theory of secondary structures described in this paper is valid in the weak segregation limit (see condition 42). Yet these structures are also stable in the strong segregation limit (see ref 27) and of course in the intermediate regime.

Another issue is the effect of thermal fluctuations which is 2-fold: (1) direct effect of fluctuations on secondary structures; (2) their indirect effect via primary structures. The theory presented above is of the mean-field type, i.e., thermal fluctuations are entirely neglected. Hence the theory is not applicable in the fluctuation zone around the critical point ($\chi n = X^*$) where a different approach[4] must be used. However thermal fluctuations affect primary morphologies only: below we show that direct effect of fluctuations on secondary structures is always negligible (even in the weak segregation limit). Therefore the theory can be generalized to the fluctuation zone in a straightforward way. One just has to change two input parameters related to primary morphologies which have to be calculated using the fluctuation approaches:[4,36,40] the mean square amplitude of primary composition modulations (parameter h) and the interfacial tension between relevant primary morphologies (parameter σ). The latter (tension) has been calculated for the transition between disordered and lamellar (primary) structures in the fluctuation zone.[36]

We comment that the theoretical approach developed in ref 36 is not entirely rigorous. The approximations involved are not really important for $\sigma_{||}$ (lamellae parallel to the interface): the numerical prefactor only is likely to be affected. However the predicted strong anisotropy of the interfacial tension ($\sigma_\perp \ll \sigma_{||}$) does not seem to be true in the fluctuation zone (although it is true in the mean-field regime, for another, cyl/lam, morphological transition as shown in section 3). Low $\sigma_\perp/\sigma_{||}$ is a consequence of the special structure of the effective Hamiltonian (see eq 19) which implies that it is the quadratic term only that is essentially wavevector dependent. This approximation is not valid in the fluctuation zone: here the fluctuation contribution to the Hamiltonian both essentially involves higher orders and is essentially wavevector dependent with the characteristic scale of the order of the correlation length $\xi \sim R_n n^{1/6}$. Hence both || and $\perp$ interfacial thicknesses are likely to be of the same order, and the same should be true for the interfacial tensions (a relevant comment can be also found in ref 41).

Let us estimate the effect of thermal fluctuations on the secondary structure. The relevant quantity is the free energy increment, ΔF, associated with a considerable shape change of one secondary domain (for simplicity we assume spherical secondary morphology here; the scaling estimates do not depend on the morphology). It is the interfacial and nonlocal (excess) free energy terms that contribute to ΔF: the total *local* free energy is independent of the secondary domain structure (see section 4). Hence ΔF must be of order of the interfacial energy increase, i.e., $\Delta F \sim \sigma\Lambda^2$ as $\Lambda^2 \sim R^2$ is the typical interfacial area per one secondary domain (at equilibrium nonlocal free energy is balanced with the interfacial term, hence nonlocal contribution is of the same order). Recalling that $\sigma \sim (k_B T/nv)R_n\epsilon^3$ (see eq 29) and $\Lambda \sim \Lambda_0 \sim R_n\epsilon^{-5/3}\delta^{-2/3}$ (see eq 43), we get $\Delta F/(k_B T) \sim (n^{1/2}a^3/v)\epsilon^{-1/3}\delta^{-4/3}$, i.e., $\Delta F \gg k_B T$. Therefore thermal fluctuations (their typical energy being $k_B T$) of the domain shape must be small, i.e., their effect on the secondary structure is always negligible.

It might be worth noting at this point that there is another source of fluctuations related to structural

heterogeneity of multiblock copolymers, i.e., polydispersity. However the "disordering" effect of polydispersity is similar to that of thermal fluctuations and hence it is not important as long as domain structure can be smoothly adjusted to the polydispersity effect which is true for block copolymers as their domains are much larger than monomer size.

We showed that the width of the secondary structure stability windows is proportional to the polydispersity degree. The secondary structures are always well-defined (strong): the secondary domain size Λ is much larger than the thickness ξ of interfacial layers between the domains. The domain size is very sensitive to the polydispersity degree δ ($\Lambda \propto \delta^{-2/3}$) and to the parameter τ (reduced temperature): Λ strongly increases as τ tends to a boundary of the stability window. The secondary domains are much larger than primary ones.

The secondary *morphology* is determined by the volume fraction p occupied by one of the competing primary structures (p is changing nearly linearly from 0 to 1 as τ varies from one boundary of the stability window to another). We found the following equilibrium secondary superstructures for the dis/bcc primary transition: lamellae (for $0.323 < p < 0.677$), hexagonal array of cylindrical domains ($0.174 < p < 0.323$, $0.677 < p < 0.826$), face centered cubic (fcc) array of spherical domains ($p < 0.174$, $p > 0.826$). Other structures including bicontinuous (double diamond and gyroid) have been also checked but were found to be unstable; i.e., their free energy is always higher than that of one of the structures listed above. The following secondary structures are predicted in the stability window corresponding to the transition between cylindrical and lamellar primary morphologies: lamellar and 3d periodic fcc array of anisotropic disks which are perforated by primary cylinders or lamellar sheets. The latter morphology is stable only if p is small or is close to 1. We did not consider secondary morphologies corresponding to transition between bcc spherical and cylindrical primary morphology. The corresponding analysis is more complicated as the interfacial tension anisotropy is neither weak nor strong in this regime.

In this paper we studied the limit of infinitely long multiblock copolymer chains. The theory is valid if the Gaussian chain size, $R = R_n m^{1/2}$ (here m is the number of blocks per chain) is much larger than the secondary domain size Λ. Using eq 43 valid for the dis/bcc window of secondary structures, we get the following condition of validity of the theory:

$$m \gg \delta^{-4/3}\epsilon^{-10/3}$$

This condition is weaker for higher polydispersity degree δ and higher compositional asymmetry ϵ. In the case of moderate polydispersity ($\delta \sim 1$) and in the intermediate segregation regime ($\epsilon \sim 1$) the secondary structures are likely to be stable with only a few blocks per chain. We also expect that it is this regime that is most favorable for experimental observation of secondary structures.

As for an experimental verification of the predicted structures, we are not aware of any direct observation of relevant secondary morphologies in multiblock copolymers. One difficulty might be related to the fact that many blocks per chain are required for the two structural levels to be distinct, thus implying very high polymer molecular weights and very slow dynamics in the case of long blocks. Shorter blocks would require stronger monomer interaction (higher χ-parameter) for the primary structure to be formed. A relevant example here is an ionomer: even short ionic blocks can form microdomains—multiplets.[44] Secondary structural elements in ionomers are known as clusters.[45] It is possible that clusters are formed according to the mechanism considered in the present paper since ionomers are in fact copolymers with polydisperse blocks.

Superstructures in block copolymers with several levels of order over different length scales has been observed recently.[46,47] Note however that these structures are due to the specific nature of some of the polymer blocks, e.g., rodlike vs flexible blocks, or blocks modified by hydrogen bonding with surfactants. Hence multiple levels of structuring in these systems are related to multiple relevant geometrical scales of polymer units and their competing interactions. On the other hand the basic units (blocks) of copolymers considered in the present paper are characterized by a single scale, their Gaussian size, which is nearly the same for all blocks.

A separate issue is the kinetic accessibility of secondary structures. This problem will be addressed separately. Here we only mention the main conclusion: the regime where equilibrium consideration is relevant does exist and is rather wide.

It is known that microphase separation in random heteropolymers might be preempted by the transition to a nonergodic "glassy" state.[42,43] However it was argued[43] that the "glass" transition temperature must be rather low with only two kinds of monomers (A and B) and with flexible polymer chains, i.e., the "glassy" state is not competitive near the critical point corresponding to formation of microdomains. In any case the effects of nonergodicity are never important for weak (primary) structures: nonergodic "glassy" structures are always strong.

Final note: secondary structures are generally incommensurable with the underlying primary structures. Hence a quantization of the secondary period Λ is possible, in particular, in the regime where Λ is not much longer than the primary domain size L (i.e., when both δ and ϵ are not too small). However these incommensurate effects are totally negligible in the weak segregation/weak polydispersity regime ($\epsilon \ll 1$, $\delta \ll 1$) considered in the present paper: here the inequalities $\Lambda \ll L \ll \xi$ ensure that the dependence of, say, interfacial tension σ on the secondary domain size is exponentially weak (in the mean-field approximation).

Appendix A. Free Energy of the Lamellar Structure

Let us calculate the nonlocal free energy, i.e., the first term F_{nloc} in the right-hand side of eq 44 (note that "tilde" is omitted below), for lamellar secondary structure. The problem is essentially one-dimensional, so we consider only one coordinate x (x-axis normal to the layers)

$$F_{\text{nloc}} = \frac{1}{2\Lambda^4}\sum_{q,q'}\frac{|\varphi_q|^2\,|\varphi_{q'}|^2}{q^2 + q'^2} \qquad \text{(A1)}$$

where $\varphi_q = \int_{-\Lambda/2}^{\Lambda/2}\varphi(x)\,dx$, Λ is the period of the structure, and the wavenumbers run over all values $q = 2\pi n/\Lambda$ with integer n, $n \neq 0$ (similarly for q'). The second-order parameter function (see eq 40) can be

defined within one period ($-\Lambda/2 < x < \Lambda/2$) as $\varphi(x) = -p + H(R - |x|)$, where $H(\cdot)$ is the Heaviside function and $R = p\Lambda/2$, so that $\varphi_q = 2\sin(qR)/q$. So we get

$$F_{\text{nloc}} = \frac{\Lambda^2}{2\pi^6} S(\pi p) \tag{A2}$$

where

$$S(\alpha) = \sum_{n=1}^{\infty}\sum_{n'=1}^{\infty} \frac{1}{n^2 + n'^2} \frac{\sin^2(\alpha n)\sin^2(\alpha n')}{n^2 n'^2}$$

Evaluating the second sum (over n') we obtain

$$S(\alpha) = \frac{1}{12}\alpha^3(\pi - \alpha)^3 - \frac{\pi}{2}\sum_{n=1}^{\infty}\frac{\sin^2(\alpha n)\sinh[(\pi - \alpha)n]\sinh(\alpha n)}{n^5 \sinh(\pi n)} \tag{A3}$$

Substituting eq A3 into eq A2 and adding the interfacial term $2/\Lambda$ (area $A = 2$ per volume $V = \Lambda$), we get eq 45 with $K_1(p) \equiv S(\pi p)/(2\pi^6)$. To find the asymptotic behavior of $S(\alpha)$ for small $\alpha \ll 1$, we write $S(\alpha) = S_0(\alpha) + S_1(\alpha) + S_2(\alpha)$, where $S_0(\alpha) = (1/2)\alpha^3(\pi - \alpha)^3$

$$S_1(\alpha) = \pi\sum_{n=1}^{\infty}\frac{\sin^2(\alpha n)\sinh^2(\alpha n)}{n^5(\exp(2\pi n) - 1)} \simeq \pi\alpha^4\sum_{n=1}^{\infty}\frac{1}{n}\frac{1}{\exp(2\pi n) - 1} \simeq 0.005883\alpha^4 \tag{A4}$$

and

$$S_2(\alpha) = -(\pi/4)\sum_{n=1}^{\infty}\frac{\sin^2(\alpha n)}{n^5}(1 - \exp(-2\alpha n)) \simeq -\frac{\pi}{4}\alpha^4 I - \frac{\pi}{4}\alpha^2 S'(\alpha) \tag{A5}$$

Here

$$I = \int_0^{\infty}\frac{\sin^2 x - x^2}{x^5}(1 - \exp(-2x))\,dx = \frac{2}{3}\ln 2 - \frac{7}{6}$$

$$S'(\alpha) = \sum_{n=1}^{\infty}\frac{1 - \exp(-2\alpha n)}{n^3} = 2\alpha^2\left(\ln(2\alpha) - \frac{3}{2}\right) + \frac{\pi^2}{3}\alpha$$

Using eqs A2−A5, we get $F_{\text{nloc}} = \Lambda^2 K_1(p)$

$$K_1(p) \simeq \frac{p^4}{4\pi}\left(\ln\frac{1}{p} - 1.5526\right) \quad \text{for} \quad p \ll 1 \tag{A6}$$

Appendix B. Nonlocal Free Energy: Spherical Morphologies

Let us consider a spherical secondary morphology: nearly spherical bcc domains forming a 3d periodic supercrystalline array. Let us start with simple cubic arrangement of the domains: the volume of one sphere $V_0 = 4\pi R^3/3 = p\Lambda^3$, where $V = \Lambda^3$ is the volume of one elementary cell, and Λ is the period in all three directions. The nonlocal free energy can be written as (again "tilde" is omitted):

$$F_{\text{nloc}} = \frac{1}{2V^4}\sum_{q\neq 0, q'\neq 0}\frac{|\varphi_q|^2\,|\varphi_{q'}|^2}{q^2 + q'^2} \tag{B1}$$

where (we assume that bcc domain is located in the center $r = 0$ of the elementary cell)

$$\varphi_q = \int_{|r|<R} e^{-i\mathbf{qr}}\,d^3r \tag{B2}$$

and $\mathbf{q} = 2\pi\mathbf{n}/\Lambda$ with $\mathbf{n}$ running over all integer 3d vectors $\mathbf{n} = (n_x, n_y, n_x)$; $\mathbf{q}'$ is running over the same set. Equation B2 follows from the definition: $\varphi_q = \int_{\text{cell}}\varphi(r)e^{-i\mathbf{qr}}\,d^3r$ (with $\varphi(r)$ defined in eq 40), and it is valid if $q \neq 0$. For $q = 0$ eq B2 implies $\varphi_{q=0} = V_0$ instead of correct $\varphi_{q=0} = 0$. However it is eq B2 that is treated below as definition of φ_q, which is acceptable since $q = 0$ is excluded from the sum in eq B1 anyway.

We then rewrite eq B1 as

$$F_{\text{nloc}} = F_1 - F_2 \tag{B3}$$

where

$$F_1 = \frac{1}{2V^4}\sum_{(q,q')\neq 0}\frac{|\varphi_q|^2|\varphi q'|^2}{q^2 + q'^2} \tag{B4}$$

$$F_2 = \frac{V_0^2}{V^4}\sum_{q\neq 0}\frac{|\varphi_q|^2}{q^2} \tag{B5}$$

and $(q, q') \neq 0$ means that either q or q' is nonzero. Next we split each term in two: $F_1 = F_{10} + F_{11}$ and $F_2 = F_{20} + F_{21}$ where F_{10} is the integral corresponding to the sum in eq B4:

$$F_{10} = \frac{1}{2V^2}\int\frac{|\varphi_q|^2\,|\varphi_{q'}|^2}{q^2 + q'^2}\frac{d^3q}{(2\pi)^3}\frac{d^3q'}{(2\pi)^3} \tag{B6}$$

and

$$F_{11} = \frac{1}{2V^4}\tilde{\sum_{(q,q')\neq 0}}\frac{|\varphi_q|^2\,|\varphi_{q'}|^2}{q^2 + q'^2}$$

is the remainder; the terms F_{20} and F_{21} have similar meaning, i.e.

$$F_{20} = \frac{V_0^2}{V^3}\int\frac{|\varphi_q|^2}{q^2}\frac{d^3q}{(2\pi)^3} \tag{B7}$$

and

$$F_{21} = \frac{V_0^2}{V^4}\tilde{\sum_{q\neq 0}}\frac{|\varphi_q|^2}{q^2}$$

Here $\tilde{\Sigma}$ means a regularized sum, i.e., the sum minus the corresponding integral. Both regularized sums are essentially dominated by a few first terms corresponding to $q \sim 1/\Lambda$, $qR \sim p^{1/3} \ll 1$. The q-dependence of φ_q in

this region can be neglected (see eq B2): $\varphi_q \simeq \varphi_{q=0} = V_0$. Hence

$$F_{11} \simeq \frac{{V_0}^4}{2V^4} \tilde{\sum_{(q,q')\neq 0}} \frac{1}{q^2 + q'^2} = \frac{p^4}{2}\left(\frac{\Lambda}{2\pi}\right)^2 S_6$$

$$F_{21} \simeq \frac{{V_0}^4}{V^4} \tilde{\sum_{q\neq 0}} \frac{1}{q^2} = p^4\left(\frac{\Lambda}{2\pi}\right)^2 S_3 \qquad \text{(B8)}$$

where

$$S_6 = \tilde{\sum_{\mathbf{n}\epsilon Z^6}} \frac{1}{n^2}; \qquad S_3 = \tilde{\sum_{\mathbf{n}\epsilon Z^3}} \frac{1}{n^2} \qquad \text{(B9)}$$

Here Z is a set of all integers, and $\mathbf{n} = 0$ is excluded from both sums in eqs B9.

The sum S_3 defined in eqs B9 can be calculated using the following identities:

$$S_3 = \tilde{\sum_{n_1 n_2 n_3}} \frac{1}{{n_1}^2 + {n_2}^2 + {n_3}^3} =$$

$$2 \tilde{\sum_{n_1 n_2 n_3}} \frac{1}{(2n_1)^2 + {n_2}^2 + {n_3}^2} - \sum_{n_1 n_2 n_3} \frac{(-1)^{n_1}}{{n_1}^2 + {n_2}^2 + {n_3}^2}$$

Doing the same transformation with respect to n_2 and n_3, we relate S_3 to itself and the sums involving $(-1)^{n_1}$ like the last sum in equation above, or involving $(-1)^{n_2}$, etc. These latter sums are explicitly convergent and can be calculated numerically (the first summation of type $\sum_{n_1} (-1)^{n_1}/({n_1}^2 + \text{const})$ can be performed analytically). The same approach also works for S_6. The result is

$$S_3 \simeq -8.913\,633; \qquad S_6 \simeq -3.379\,685 \qquad \text{(B10)}$$

Doing integral in eq B2 and substituting the result

$$\varphi_q = 4\pi R^3\left[\frac{\sin(qR)}{(qR)^3} - \frac{\cos(qR)}{(qR)^2}\right]$$

in eqs B6 and B7 we get

$$F_{10} = k_{10}p^2R^2; \qquad k_{10} \simeq 0.04374; \qquad F_{20} = 0.4p^3R^2 \qquad \text{(B11)}$$

Using eqs B3, B8, B10, and B11, we get the nonlocal free energy for the simple cubic structure ($p \ll 1$)

$$F_{\text{nloc}} = R^2p^2\{k_{10} - 0.4p + sp^{4/3}\} \qquad \text{(B12)}$$

where $s = (1/8\pi^2)(4\pi/3)^{3/2}\ S_6 - 2S_3) \simeq 0.475478$.

Other secondary superlattices (bcc, fcc, hcp) can be analyzed in the same way. The free energy is still given by eq B12, but with different numerical factors: $s =$ 0.471 083 41 (bcc), 0.470 926 95 (hcp), 0.470 926 26 (fcc).

Acknowledgment. A.E.L. is supported by the Royal Society/NATO Postdoctoral Fellowship Program. A.N.S. also acknowledges partial support by the EPSRC, Grant GR/L70851.

References and Notes

(1) Matsen, M. W.; Schick, M. *Curr. Opin. Colloid Interface Sci.* **1996**, *1*, 329.
(2) Matsen, M. W.; Bates, F. S. *Macromolecules* **1996**, *29*, 1091.
(3) Leibler, L. *Macromolecules* **1980**, *13*, 1602.
(4) Fredrickson, G. H.; Helfand, E. J. Chem. Phys. **1987**, *87*, 697.
(5) Matsen, M. W.; Bates, F. S. *Macromolecules* **1996**, *29*, 7641.
(6) Zhulina, E. B.; Lyatskaya, Y. V.; Birshtein, T. M. *Polymer* **1992**, *33*, 332.
(7) Spontak, R. J. *Macromolecules* **1994**, *27*, 6363.
(8) Burger, C.; Ruland, W.; Semenov, A. N. *Macromolecules* **1990**, *23*, 3339.
(9) Erukhimovich, I. Ya.; Dobrynin, A. V. *Macromol. Symp.* **1994**, *81*, 253.
(10) Matsen, M. W. *J. Chem. Phys.* **1995**, *103*, 3268.
(11) Matsen, M. W.; Bates, F. S. *Macromolecules* **1995**, *28*, 7298.
(12) Benoit, H.; Hadziioannou, G. *Macromolecules* **1988**, *21*, 1449.
(13) Dobrynin, A. V.; Erukhimovich, I. Ya. *Macromolecules* **1993**, *26*, 276.
(14) Zielinski, J. M.; Spontak, R. J. *Macromolecules* **1992**, *25*, 653. Spontak, R. J.; Zielinski, J. M.; Lipscomb, G. G. *Macromolecules* **1992**, *25*, 6270. Spontak, R. J.; Smith, S. D.; Ashraf, A. *Macromolecules* **1993**, *26*, 5118.
(15) Matsen, M. W.; Schick, M. *Macromolecules* **1994**, *27*, 7157.
(16) Olmsted, P. D.; Milner, S. T. *Macromolecules* **1994**, *27*, 1964.
(17) Shakhnovich, E. I.; Gutin, A. M. *J. Phys. (Paris).* **1989**, *50*, 1843.
(18) Dobrynin, A. V.; Erukhimovich, I. Ya. *Sov. Phys. JETP Lett.* **1991**, *53*, 570.
(19) Fredrickson, G. H.; Milner, S. T. *Phys. Rev. Lett.* **1991**, *67*, 835.
(20) Panyukov, S. V.; Kuchanov, S. I. *J. Phys. II* **1992**, *2*, 1973.
(21) Fredrickson, G. H.; Milner, S. T.; Leibler, L. *Macromolecules* **1992**, *25*, 6341.
(22) Gutin, A. M.; Sfatos, C. D.; Shakhnovich, E. I. *J. Phys. A* **1994**, *27*, 7957.
(23) Dobrynin, A. V.; Erukhimovich, I. Ya. *J. Phys. I* **1995**, *5*, 365.
(24) Sfatos, C. D.; Gutin, A. M.; Shakhnovich, E. I. *Phys. Rev. E* **1995**, *51*, 4727.
(25) Angerman, H.; Ten Brinke, G.; Erukhimovich, I. *Macromolecules* **1996**, *29*, 3255.
(26) Angerman, H.; Ten Brinke, G.; Erukhimovich, I. *Macromolecules* **1998**, *31*, 1958.
(27) Semenov, A. N. *J. Phys. II* **1997**, *7*, 1489.
(28) Dobrynin, A. V.; Leibler, L. *Europhys. Lett.* **1996**, *36*, 283.
(29) Dobrynin, A. V.; Leibler, L. *Macromolecules* **1997**, *30*, 4756.
(30) Dobrynin, A. V. *J. Chem. Phys.* **1997**, *107*, 9234.
(31) Panyukov, S.V.; Potemkin, I. I. *JETP* **1997**, *85*, 183.
(32) Panyukov, S.; Potemkin, I. *Physica A* **1998**, *249*, 321.
(33) Potemkin, I. I.; Panyukov, S. V. *Phys. Rev. E* **1998**, *57*, 6902.
(34) Landau, L. D.; Lifshitz, E. M. *Statistical Physics*, 3rd ed., Part 1; Pergamon Press: Oxford, 1980.
(35) Fredrickson, G.; Binder, K. *J. Chem. Phys.* **1989**, *91*, 7265.
(36) Hohenberg, P. C.; Swift, J. B. *Phys. Rev. E* **1995**, *52*, 1828.
(37) Erukhimovich, I. Ya. Private communication.
(38) Fournier, J. B.; Durand, G. *J. Phys. II* **1991**, *1*, 845.
(39) Bidaux, R.; Boccara, N.; Sarma, G.; De Seze, L.; De Gennes, P. G.; Parodi, O. *J. Phys. (Paris)* **1973**, *34*, 661.
(40) Brazovskii, S. A. *Sov. Phys. JETP* **1975**, *41*, 85.
(41) Goveas, J. L.; Milner, S. T. *Macromolecules* **1997**, *30*, 2605.
(42) Grosberg, A. Yu. *Sov. Phys.—Usp. Fiz. Nauk* **1997**, *167*, 129.
(43) Sfatos, C. D.; Shakhnovich, E. I. *Phys. Rep.* **1997**, *288*, 77.
(44) Schlick, S., Ed. *Ionomers. Characterization, Theory, and Applications*; CRC Press: Boca Raton, FL, 1995.
(45) I am grateful to A. R. Khokhlov who pointed out to a possible relation between clusters and secondary structures.
(46) Muthukumar, M.; Ober, C. K.; Thomas, E. L. *Science* **1997**, *277*, 1225.
(47) Ruokolainen, J.; Mäkinen, R.; Torkelli, M.; Mäkelä, T.; Serimaa, R.; Ten Brinke, G.; Ikkala, O. *Science* **1998**, *280*, 557.

MA981044J